

# CPM Specifications Document

## Cerebrovascular Aneurysms:

OSMSC 0168\_0001, 0169\_0002, 0170\_0001, 0171\_0001, 0178\_0000, 0179\_0000, 0180\_0000,  
0181\_0000, 0182\_0000

---

May 1, 2013

Version 1

Open Source Medical Software Corporation

© 2013 Open Source Medical Software Corporation. All Rights Reserved.

# 1. Clinical Significance & Condition

Stroke is the number 4 leading cause of death in the U.S., killing more than 137,000 people a year [1]. An estimated 5-15% of stroke cases are related to intracranial aneurysm rupture [2]. If an aneurysm ruptures and subarachnoid hemorrhage occurs, risk of death is up to 45% within thirty days and risk of severe brain damage is 20 to 30% [3]. Prevalence of aneurysms is estimated in about 1% to 5% of the general population; however only a small number are symptomatic or rupture [2]. About 3 to 5 million people in the U.S have cerebral aneurysms [3].

Cerebral aneurysms usually develop after age of 40 and the incidence of subarachnoid hemorrhage from a ruptured aneurysm peaks in peoples between the ages of 55 and 60 [2, 3]. Little is known about the formation and cause of cerebral aneurysms however they frequently develop at sites where blood is most turbulent and wall shear forces are greatest [4]. Cerebral aneurysms have been associated with hypertension, smoking-induced vascular changes, drugs such as amphetamines and cocaine, brain trauma, and autosomal dominant polycystic kidney disease [3, 2].

Aneurysms can be saccular, also known as a berry aneurysm, with a well-defined neck or a wide-necked and fusiform (Figure 1) [3, 5]. They are classified by size as *small* (less than 5mm), medium (6-15mm), large (16-25 mm) and giant (larger than 25mm) [3]. The two most common sites where cerebral aneurysms form are in the anterior communicating artery and at the bifurcation of the internal carotid artery and the posterior communicating artery; 60% to 70% of aneurysms occur at those sites. Aneurysms at the middle cerebral artery bifurcation and basilar artery bifurcation are also common and most other aneurysms occur in the posterior circulation arteries [4].

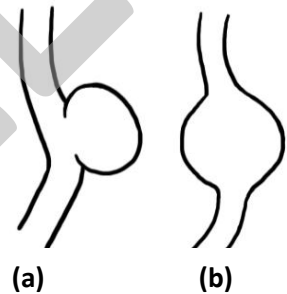


Figure 1 - wide-necked saccular (a) and fusiform (b) aneurysms

There are two main options for treating cerebral aneurysms: clipping and coiling.

Permanent clips made from MRI-compatible alloys are placed across the neck of saccular aneurysms to prevent rupture (Figure 2) [2]. If a cerebral aneurysm ruptures, it is often treated using coiling, where detachable coils of various sizes and shapes are inserted in the aneurysm to stop blood from entering the aneurysm [2]. Aneurysms treated with coiling may recur as a result of coil compression by the aneurysm, allowing blood to flow to the

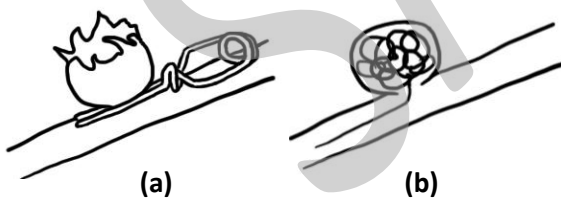


Figure 2 - Two main treatment options for cerebral aneurysms: clipping (a) and coiling (b)

aneurysm. One potential solution to recurring aneurysms is stent-assisted recoiling, where a microcatheter-delivered stent is placed in the vicinity of the aneurysm, blocking flow to the aneurysm and directing it through the artery [2]. The optimal treatment for different aneurysms remains controversial and requires further investigation. Computational Fluid Dynamics (CFD) studies may offer a noninvasive tool in assessing potential treatments and quantifying hemodynamics in cerebral aneurysms.

## 2. Clinical Data

Patient-specific volumetric image data was obtained to create physiological models and blood flow simulations. Details of the imaging data used can be seen in Table 1. See Appendix 1 for details on image data orientation.

Table 1 – Patient-specific volumetric image data details (mm)

OSMSC ID	Modality	Voxel Spacing	Voxel Dimensions	Physical Dimensions
0168_0001	CT	0.3906 x 0.3906 x 0.6250	512 x 512 x 259	200.00 x 200.00 x 161.87
0169_0002	MR	0.3125 x 0.3125 x 0.7000	512 x 512 x 156	160.00 x 160.00 x 109.20
0170_0001	MR	0.3516 x 0.3516 x 0.6000	440 x 512 x 142	154.69 x 180.00 x 85.20
0171_0001	MR	0.3516 x 0.3516 x 0.7001	512 x 512 x 144	180.02 x 180.02 x 100.81
0178_0000	MR	0.3516 x 0.3516 x 0.7000	512 x 512 x 144	180.02 x 180.02 x 100.81
0179_0000	CT	0.3906 x 0.3906 x 0.6250	512 x 512 x 267	200.00 x 200.00 x 166.87
0180_0000	CT	0.3906 x 0.3906 x 0.6250	512 x 512 x 273	200.00 x 200.00 x 170.62
0181_0000	MR	0.3125 x 0.3125 x 0.7001	512 x 512 x 156	160.00 x 160.0 x 109.21
0182_0000	MR	0.4297 x 0.4297 x 0.6000	512 x 512 x 144	220.01 x 220.01 x 86.40

Available patient-specific clinical data collected can be seen in Table 2.


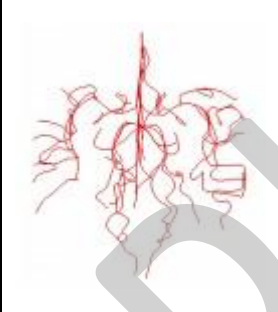
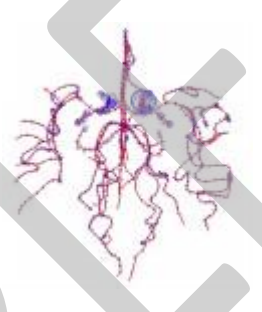
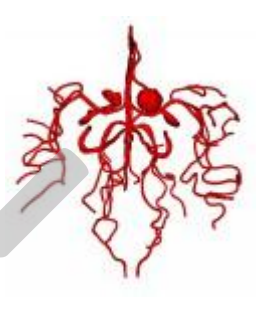
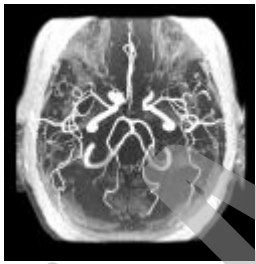

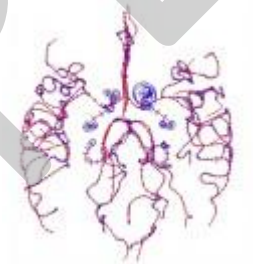



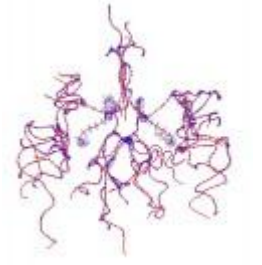
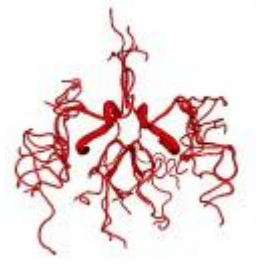

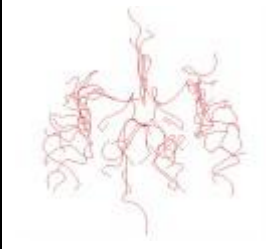
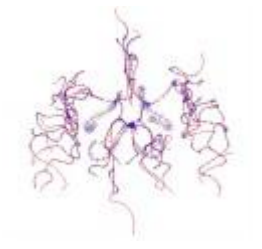
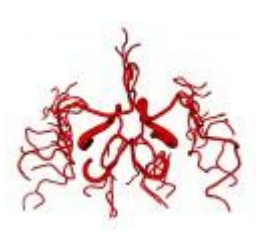
Table 2 – Available patient-specific clinical data

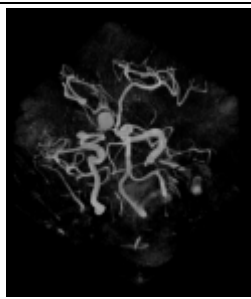

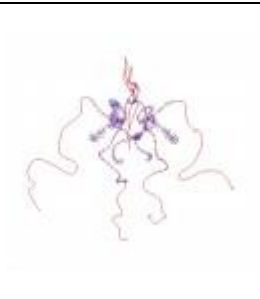

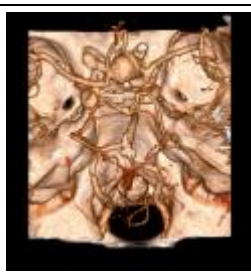

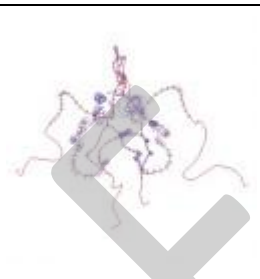



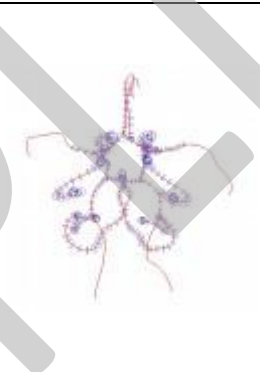
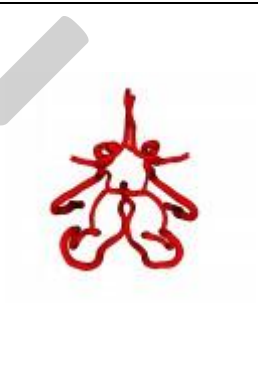
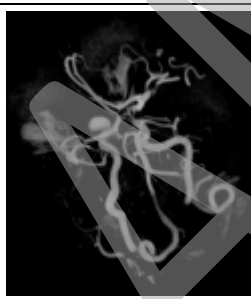

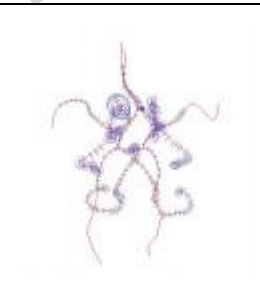

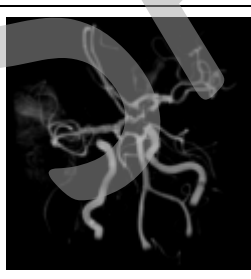
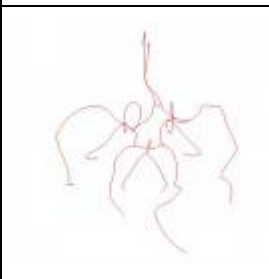
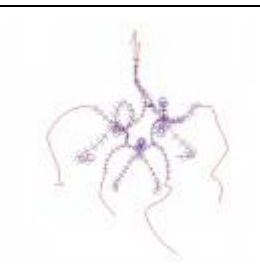

OSMSC ID	Patient	Age	Gender	Height (m)	Weight (kg)	BMI	BSA (m <sup>2</sup> )	HR (bpm)	Psys (mmHg)	Pdia (mmHg)	Pavg (mmHg)
0168_0001	1 - PreOp	47	F	1.63	46.6	29.0	1.9	92	135	74	94
0169_0002	1 - PostOp	47	F	1.63	46.6	29.0	1.9	92	135	74	94
0170_0001	2 – PreOp	69	F	1.63	90.7	34.3	2.0	79	161	84	79
0171_0001	2 – PostOp	69	F	1.63	90.7	34.3	2.0	79	161	84	79
0178_0000	3 – PreOp	56	F	1.73	76.7	25.7	1.9	62	136	66	94
0179_0000	4 – PreOp	39	F	1.70	121.6	42	2.4	63	114	69	89
0180_0000	4 – PostOp	39	F	1.70	121.6	42	2.4	63	114	69	89
0181_0000	5 – PreOp	32	F	1.65	61.2	22.5	1.7	67	135	91	84
0182_0000	5 – PostOp	32	F	1.65	61.2	22.5	1.7	67	135	91	84

### 3. Anatomic Model Description

Anatomic models were created using customized SimVascular software (Simtk.org) and the image data described in Section 2. The models include the Circle of Willis with various levels of branching extending off of it. See Appendix 2 for a description of modeling methods. See Table 3 for a visual summary of the image data, paths, segmentations and solid model constructed.

Table 3 – Visual summary of image data, paths, segmentations and solid model.

OSMSC ID	Image Data	Paths	Paths and Segmentations	Model
ID: OSMSC0168 subID: 0001 Age: 47 Gender: F				
ID: OSMSC0169 subID: 0002 Age: 47 Gender: F				
ID: OSMSC0170 subID: 0001 Age: 69 Gender: F				
ID: OSMSC0171 subID: 0001 Age: 69 Gender: F				

<p>ID: OSMSC0178 subID: 0000 Age: 56 Gender: F</p>				
<p>ID: OSMSC0179 subID: 0000 Age: 39 Gender: F</p>				
<p>ID: OSMSC0180 subID: 0000 Age: 39 Gender: F</p>				
<p>ID: OSMSC0181 subID: 0000 Age: 32 Gender: F</p>				
<p>ID: OSMSC0182 subID: 0000 Age: 32 Gender: F</p>				

Details of anatomic models, such as number of outlets and model volume, can be seen in Table 4.

Table 4 – Anatomic Model details

OSMSC ID	Inlets	Outlets	Volume (cm <sup>3</sup> )	Surface Area (cm <sup>2</sup> )	Vessel Paths	2-D Segmentations
0168_0001	4	32	8.627919	147.458163	36	919
0169_0002	4	46	8.320261	163.526791	53	1386
0170_0001	4	45	7.750584	150.104515	48	1496
0171_0001	4	49	8.149295	139.313589	52	1268
0178_0000	4	6	4.20202	54.0957	12	243
0179_0000	4	6	7.20259	82.6403	12	341
0180_0000	4	6	5.971958	72.863607	11	292
0181_0000	4	6	6.447057	69.116603	12	268
0182_0000	4	6	3.666779	45.300526	10	185

## 4. Physiological Model Description

In addition to the clinical data gathered for this model, several physiological assumptions were made in preparation for running the simulation. See Appendix 3 for details.

## 5. Simulation Parameters & Details

No simulation results available.

## 6. Simulation Results

No simulation results available.

## 7. References

- [1] American Stroke Association, "Impact of," 6 March 2012. [Online]. Available: [http://www.strokeassociation.org/STROKEORG/AboutStroke/Impact-of-Stroke\\_UCM\\_310728\\_Article.jsp#.T3tvM6t8B8E](http://www.strokeassociation.org/STROKEORG/AboutStroke/Impact-of-Stroke_UCM_310728_Article.jsp#.T3tvM6t8B8E). [Accessed 3 April 2012].
- [2] J. L. Brisman, J. K. Song and D. W. Newell, "Cerebral Aneurysms," *The New England Journal of Medicine*, vol. 355, no. 9, pp. 928-939, 2006.
- [3] American Stroke Association, "What You Should Know About Cerebral Aneurysms," 22 June 2011. [Online]. Available: [http://www.strokeassociation.org/STROKEORG/AboutStroke/TypesofStroke/What-You-Should-Know-About-Cerebral-Aneurysms\\_UCM\\_310103\\_Article.jsp#.T3tweqt8B8E](http://www.strokeassociation.org/STROKEORG/AboutStroke/TypesofStroke/What-You-Should-Know-About-Cerebral-Aneurysms_UCM_310103_Article.jsp#.T3tweqt8B8E). [Accessed 3 April 2012].
- [4] C. Vega, J. Kwoon and S. Lavine, "Intracranial Aneurysms: Current Evidence and Clinical practice," *American Family Physician*, vol. 66, no. 4, pp. 601-609, 2002.



[5] Yale Medical Group, "Endovascular Coiling," 2012. [Online]. Available:  
<http://www.yalemedicalgroup.org/stw/Page.asp?PageID=STW029076>. [Accessed 25 May 2012].

SAMPLE

## Appendix

### 1. Image Data Orientation

The RAS coordinate system was assumed for the image data orientation. Voxel Spacing, voxel dimensions, and physical dimensions are provided in the Right-Left (R), Anterior-Posterior (A), and Superior-Inferior (S) direction in all specification documents unless otherwise specified.

### 2. Model Construction

All anatomic models were constructed in RAS Space. The models are generated by selecting centerline paths along the vessels, creating 2D segmentations along each of these paths, and then lofting the segmentations together to create a solid model. A separate solid model was created for each vessel and Boolean addition was used to generate a single model representing the complete anatomic model. The vessel junctions were then blended to create a smoothed model.

### 3. Physiological Assumptions

Newtonian fluid behavior is assumed with standard physiological properties. Blood viscosity and density are given below in units used to input directly into the solver.

**Blood Viscosity:**  $0.04 \text{ g/cm} \cdot \text{s}^2$

**Blood Density:**  $1.06 \text{ g/cm}^3$

### 4. Simulation Parameters

Conservation of mass and Navier-Stokes equations were solved using 3D finite element methods assuming rigid and non-slip walls. All simulations were ran in cgs units and ran for several cardiac cycles to allow the flow rate and pressure fields to stabilize.

### 5. Outlet Boundary Conditions

#### 5.1 Resistance Methods

Resistances values can be applied to the outlets to direct flow and pressure gradients. Total resistance for the model is calculated using relationships of the flow and pressure of the model. Total resistance is than distributed amongst the outlets using an inverse relationship of outlet area and the assumption that the outlets act in parallel.

#### 5.2 Windkessel Model

In order to represent the effects of vessels distal to the CFD model, a three-element Windkessel model can be applied at each outlet. This model consists of proximal resistance ( $R_p$ ), capacitance ( $C$ ), and distal resistance ( $R_d$ ) representing the resistance of the proximal vessels, the capacitance of the proximal vessels, and the resistance of the distal vessels downstream of each outlet, respectively (Figure 1).

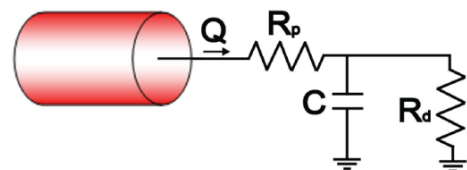


Figure 3 - Windkessel model



First, total arterial capacitance (TAC) was calculated using inflow and blood pressure. The TAC was then distributed among the outlets based on the blood flow distributions. Next, total resistance ( $R_t$ ) was calculated for each outlet using mean blood pressure and PC-MRI or calculated target flow ( $R_t = P_{\text{mean}} / Q_{\text{desired}}$ ). Given that  $R_t = R_p + R_d$ , total resistance was distributed between  $R_p$  and  $R_d$  adjusting the  $R_p$  to  $R_t$  ratio for each outlet.

SAMPLE